



## Magnetically activated microcapsules as controlled release carriers for a liquid PDMS cross-linker

Kostrzewska, Malgorzata; Yu, Liyun; Li, Yang; Li, Jiansheng; Wenzell, Berit; Kasama, Takeshi; Skov, Anne Ladegaard

*Published in:*  
Materials Research Express

*Link to article, DOI:*  
[10.1088/2053-1591/aae913](https://doi.org/10.1088/2053-1591/aae913)

*Publication date:*  
2019

*Document Version*  
Peer reviewed version

[Link back to DTU Orbit](#)

*Citation (APA):*  
Kostrzewska, M., Yu, L., Li, Y., Li, J., Wenzell, B., Kasama, T., & Skov, A. L. (2019). Magnetically activated microcapsules as controlled release carriers for a liquid PDMS cross-linker. *Materials Research Express*, 6(1), [015310]. <https://doi.org/10.1088/2053-1591/aae913>

---

### General rights

Copyright and moral rights for the publications made accessible in the public portal are retained by the authors and/or other copyright owners and it is a condition of accessing publications that users recognise and abide by the legal requirements associated with these rights.

- Users may download and print one copy of any publication from the public portal for the purpose of private study or research.
- You may not further distribute the material or use it for any profit-making activity or commercial gain
- You may freely distribute the URL identifying the publication in the public portal

If you believe that this document breaches copyright please contact us providing details, and we will remove access to the work immediately and investigate your claim.

ACCEPTED MANUSCRIPT

# Magnetically activated microcapsules as controlled release carriers for a liquid PDMS cross-linker

To cite this article before publication: Malgorzata Kostrzevska *et al* 2018 *Mater. Res. Express* in press <https://doi.org/10.1088/2053-1591/aae913>

## Manuscript version: Accepted Manuscript

Accepted Manuscript is “the version of the article accepted for publication including all changes made as a result of the peer review process, and which may also include the addition to the article by IOP Publishing of a header, an article ID, a cover sheet and/or an ‘Accepted Manuscript’ watermark, but excluding any other editing, typesetting or other changes made by IOP Publishing and/or its licensors”

This Accepted Manuscript is © 2018 IOP Publishing Ltd.

During the embargo period (the 12 month period from the publication of the Version of Record of this article), the Accepted Manuscript is fully protected by copyright and cannot be reused or reposted elsewhere.

As the Version of Record of this article is going to be / has been published on a subscription basis, this Accepted Manuscript is available for reuse under a CC BY-NC-ND 3.0 licence after the 12 month embargo period.

After the embargo period, everyone is permitted to use copy and redistribute this article for non-commercial purposes only, provided that they adhere to all the terms of the licence <https://creativecommons.org/licenses/by-nc-nd/3.0>

Although reasonable endeavours have been taken to obtain all necessary permissions from third parties to include their copyrighted content within this article, their full citation and copyright line may not be present in this Accepted Manuscript version. Before using any content from this article, please refer to the Version of Record on IOPscience once published for full citation and copyright details, as permissions will likely be required. All third party content is fully copyright protected, unless specifically stated otherwise in the figure caption in the Version of Record.

View the [article online](#) for updates and enhancements.

1  
2  
3 **Magnetically activated microcapsules as controlled release carriers for a liquid**  
4  
5 **PDMS cross-linker**  
6  
7  
8  
9

10  
11 **Malgorzata Kostrzevska<sup>1</sup>, Liyun Yu<sup>1</sup>, Yang Li<sup>2</sup>, Jiansheng Li<sup>2</sup>, Berit Wenzell<sup>3</sup>, Takeshi**  
12  
13 **Kasama<sup>3</sup>, Anne Ladegaard Skov<sup>1\*</sup>**  
14

15 <sup>1</sup> Danish Polymer Centre, Department of Chemical and Biochemical Engineering, Technical  
16 University of Denmark, Søltofts Plads Building 227, 2800 Kgs. Lyngby, Denmark  
17  
18

19 <sup>2</sup> Jiangsu Key Laboratory of Chemical Pollution Control and Resources Reuse, School of  
20 Environmental and Biological Engineering, Nanjing University of Science and Technology,  
21  
22 210094 Nanjing, P. R. China  
23  
24  
25

26 <sup>3</sup> Center for Electron Nanoscopy, Technical University of Denmark, Fysikvej 307, 2800 Kgs.  
27 Lyngby, Denmark  
28  
29

30  
31 \*Corresponding author: Tel.: +45 45252825. Fax: +45 45882258. E-mail: al@kt.dtu.dk  
32  
33  
34  
35

36 **Abstract**  
37

38 Injecting water into a porous oil reservoir enhances oil sweep efficiency and leads to increased  
39 oil production, but due to the occurrence of fractures in water-flooded reservoirs, excessive  
40 water production is observed. Hence, water shut-off treatments are continuously investigated,  
41 albeit currently applied plugging materials still suffer from some disadvantages such as lack of  
42 selectivity and poor mechanical strength. In this work, we introduce a new plugging material  
43 consisting of vinyl-functional PDMS microspheres and magnetically activated microcapsules.  
44  
45 This work focuses on the preparation and characterisation of microcapsules containing  
46 magnetite nanoparticles (MNPs), and liquid cross-linker in their core. The microcapsules are  
47 prepared via a phase separation technique, and it is established that the MNPs are located inside  
48  
49 the microcapsules and that the shell remains nonporous, in which case the cross-linker is well  
50  
51  
52  
53  
54  
55  
56  
57  
58  
59  
60

1  
2  
3 protected before activating the microcapsules. While exposed to an alternating magnetic field,  
4  
5 the MNPs generate sufficient heat to soften the polymeric shell, thereby leading to the efficient  
6  
7 release of the cross-linker; moreover, the PDMS microspheres create a strong network, due to  
8  
9 a cross-linking reaction. It is expected that this new approach will improve significantly the  
10  
11 plugging process of fractures in matured reservoirs, which in turn will lead to higher oil  
12  
13 recovery rates.  
14  
15

16 **Keywords:** alternating magnetic field, magnetically activated microcapsules, PDMS  
17  
18 microspheres, liquid cross-linker, magnetite  
19  
20  
21  
22  
23

## 24 **1. Introduction**

25  
26 Water-flooding treatment is applied when underground pressure in oil reservoirs drops notably  
27  
28 and becomes insufficient to drive the oil to the surface. In this method, water is injected into  
29  
30 porous reservoir rock to displace the oil and push it towards the production well [1,2], thereby  
31  
32 increasing the pressure of the reservoir, which can be maintained for a long time. An illustration  
33  
34 of the water flooding method is presented in **Figure 1a**. However, naturally occurring fractures  
35  
36 decrease oil production because the injected water passes easily through fractures, leaving  
37  
38 unswept oil in low-permeable, porous zones (**Figure 1b**). It is evident that in order to maintain  
39  
40 oil production, the fractures need to be shut off to water (**Figure 1c**) [3]. Since successful  
41  
42 fracture plugging in water-flooded oil reservoirs significantly increases oil recovery rates,  
43  
44 relevant methods are being improved constantly.  
45  
46  
47  
48  
49  
50  
51  
52  
53  
54  
55  
56  
57  
58  
59  
60

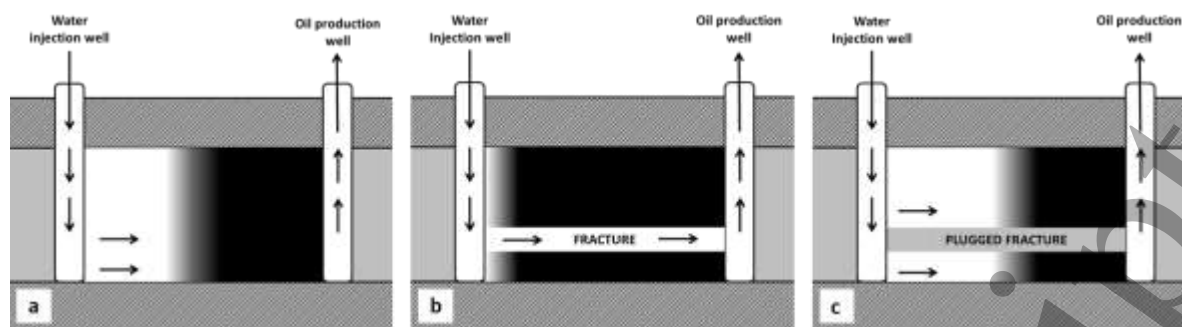


**Figure 1.** Illustration of a proposed water injection method in an oil reservoir. **a)** As fractures are not present in the reservoir, oil production is high due to a sufficient pressure difference. **b)** The presence of fractures leads to lower oil production, as water passes through the fracture easily. **c)** Plugging the fracture results in satisfactory oil production. White and black colours represent water and oil flows in the reservoir, respectively.

Nowadays, water shut-off is achieved mainly by injecting highly swellable polymeric hydrogels [4-8]. The most commonly used hydrogels can be divided into three main categories: inorganic gels (e.g. sodium silicate gel), polymer-based gels (e.g. acrylamide monomer-based and polyacrylamide gels) and preformed particle gels (PPG). The swollen gels show fairly good elastic properties and are capable of withstanding high pressures [9]. However, this technique suffers from some disadvantages. The hydrogels are injected into the reservoir in the form of low-viscosity mixtures, and although the swelling can be controlled to some extent, the hydrogels often start swelling well before placing the material inside the fracture, thus blocking the injection well. Moreover, polymer chains in the hydrogels are not covalently bonded, as they only swell and do not react chemically with each other, which causes poor set plug mechanical strength. Finally, due to the low viscosity of the mixtures, the hydrogel may seep into oil-rich pores and plug the whole reservoir, not only the fracture.

Poly(dimethylsiloxane) (PDMS) is the most commonly used of the polymeric organosilicon compounds, generally referred to as silicones, and it has been chosen for this

1  
2  
3 work because of its unique properties, such as highly elasticity and excellent compressibility,  
4 hydrophobicity and outstanding resistance to oil at high temperatures [10]. The plugging  
5 material consists of vinyl-functional PDMS microspheres and magnetically activated  
6 microcapsules with a hydride cross-linker. After the cross-linker is released from the  
7 microcapsules, PDMS microspheres can be bonded covalently with each other through the  
8 hydrosilylation reaction [11].  
9

10  
11 This work deals with designing a novel plugging material that blocks fractures selectively  
12 and efficiently in a controllable way compared to the known plugging materials, i.e. hydrogels.  
13 PDMS is injected into the fracture in the form of pre-crosslinked microparticles, which do not  
14 swell in contact with water, and hence the danger of blocking the injection well, due to the  
15 premature swelling of the particles, is eliminated. The size of the PDMS microparticles can be  
16 designed to be smaller than the fracture width but larger than the pore diameter. In this way,  
17 the material will enter in the fracture only, without blocking the pores. As the PDMS particles  
18 are less deformable than hydrogels, they will not penetrate into pores even under high pressure.  
19 Moreover, the PDMS microparticles have reactive vinyl groups on the surface. These vinyl  
20 groups are capable of further reacting with the multi-functional crosslinker. After the reaction  
21 inside the fracture, each microparticle is covalently connected with other microparticles by a  
22 cross-linker, and a strong barrier is created. This makes the material even more durable and  
23 resistant to high pressure. In this way, the macroscopic PDMS elastomer cannot be washed  
24 away due to the injection of water and should cause long-term durability of the treatment.  
25  
26  
27  
28  
29  
30  
31  
32  
33  
34  
35  
36  
37  
38  
39  
40  
41  
42  
43  
44  
45  
46  
47  
48

49 An alternating magnetic field (AMF) is applied as an activating stimulus in this study, as it  
50 easily penetrates the materials and can be applied from a distance. When magnetic materials,  
51 for example magnetic nanoparticles, are subjected to AMF, they generate heat due to heat  
52 dissipation caused by the delay in relaxing the magnetic moment through either rotation within  
53 the particle (Néel mechanism) or rotation of the particle itself (Brownian mechanism) [12-14].  
54  
55  
56  
57  
58  
59  
60

1  
2  
3 Magnetic material heating by AMF is used in many industrial processes, such as heat treatment  
4 in metallurgy and to melt refractory metals, which require very high temperatures [15]. The  
5 most commonly used magnetic nanoparticles are made from iron oxide, called magnetite [16],  
6 which contains both ferrous and ferric iron species [17,18]. Magnetic relaxation of magnetite  
7 is exploited in innovative biomedical magnetic particle applications such as magnetic particle  
8 imaging [19], magnetic fluid hyperthermia [20] and biosensing [21]. In this study, magnetite  
9 nanoparticles (MNPs) without and with non-reactive PDMS surface modifications were  
10 subjected to AMF, and their heating properties were examined. Subsequently, microcapsules  
11 with MNPs, which can be activated by applying the AMF, were prepared and characterised.  
12 The release of the cross-linker was expected after subjecting the microcapsules to AMF. The  
13 hypothesis is that at certain frequencies, MNPs generate enough heat to break microcapsules  
14 above the shell's glass transition temperature ( $T_g$ ).  
15  
16  
17  
18  
19  
20  
21  
22  
23  
24  
25  
26  
27  
28  
29  
30  
31  
32

## 33 **2. Experimental**

### 34 **2.1. Materials**

35  
36 A hydride-functional cross-linker (HMS-301,  $M_w=2000$  g/mol), vinyl-terminated  
37 poly(dimethylsiloxane) DMS-V22 ( $M_w=9400$  g/mol) and DMS-V31 ( $M_w=28000$  g/mol) were  
38 purchased from Gelest. Poly(vinyl alcohol) (PVA,  $M_w=22000$  g/mol), used as an emulsifier,  
39 was purchased from Fluka. Platinum cyclovintlmethyl siloxane complex Catalyst 511 was  
40 obtained from Hanse Chemie, whereas Inhibitor PT88 was purchased from Wacker Chemie.  
41 Poly(methyl methacrylate) (PMMA,  $M_w=15000$  g/mol), non-reactive silicone oil (methyl-  
42 terminated poly(dimethylsiloxane)) with viscosity 20 cSt, sodium dodecyl sulfate (SDS),  
43 dichloromethane (DCM) and deuterated chloroform ( $CDCl_3$ ) were acquired from Sigma-  
44 Aldrich.  
45  
46  
47  
48  
49  
50  
51  
52  
53  
54  
55  
56  
57  
58  
59  
60

1  
2  
3 Magnetic nanoparticles  $\text{Fe}_3\text{O}_4$  and  $\text{Fe}_3\text{O}_4$ -PDMS, with a diameter of approximately 50 nm,  
4  
5 were synthesised according the reported reference [22], and the experimental details are  
6  
7 presented in electronic supplementary information (ESI).  
8  
9

## 10 11 12 **2.2. Preparation of magnetic microcapsules**

13  
14 The preparation of microcapsules with a PMMA shell and a liquid cross-linker as a core was  
15  
16 studied extensively in our previous work [23,24], that is microcapsules with a silicone oil core  
17  
18 (methylhydrosiloxane-dimethylsiloxane, HMS-301) surrounded by a polymeric shell, PMMA  
19  
20 was synthesized by the controlled phase separation of a polymer dissolved within the silicone  
21  
22 oil droplets of an oil-in-water emulsion. The phase separation technique in this work, as  
23  
24 illustrated in **Figure 2**, was adapted to prepare magnetic microcapsules as follows: an oil phase  
25  
26 was prepared by adding the proper amount of the cross-linker (HMS-301) and the magnetite  
27  
28 nanoparticles to an organic solvent, preceded by dissolving PMMA. This prepared oil phase  
29  
30 was then placed in an ultrasonic bath for 2 hours, in order to obtain well dispersion of  
31  
32 nanoparticles. Afterwards, approximately 150 mL of aqueous PVA emulsifier solution was  
33  
34 charged to a 250 mL conical flask and the aqueous phase was mechanically stirred at 2000 rpm  
35  
36 for 2-5 min. The oil phase was added drop-wise over 60 s to form an oil-in-water emulsion.  
37  
38 The agitation was maintained for further 2 hours at around 750 rpm. Microcapsule dispersion  
39  
40 was filtered with a filtration pump. Finally, the product was washed with distilled water (~1.5  
41  
42 L) and dried at room temperature.  
43  
44  
45  
46  
47  
48  
49  
50  
51  
52  
53  
54  
55  
56  
57  
58  
59  
60



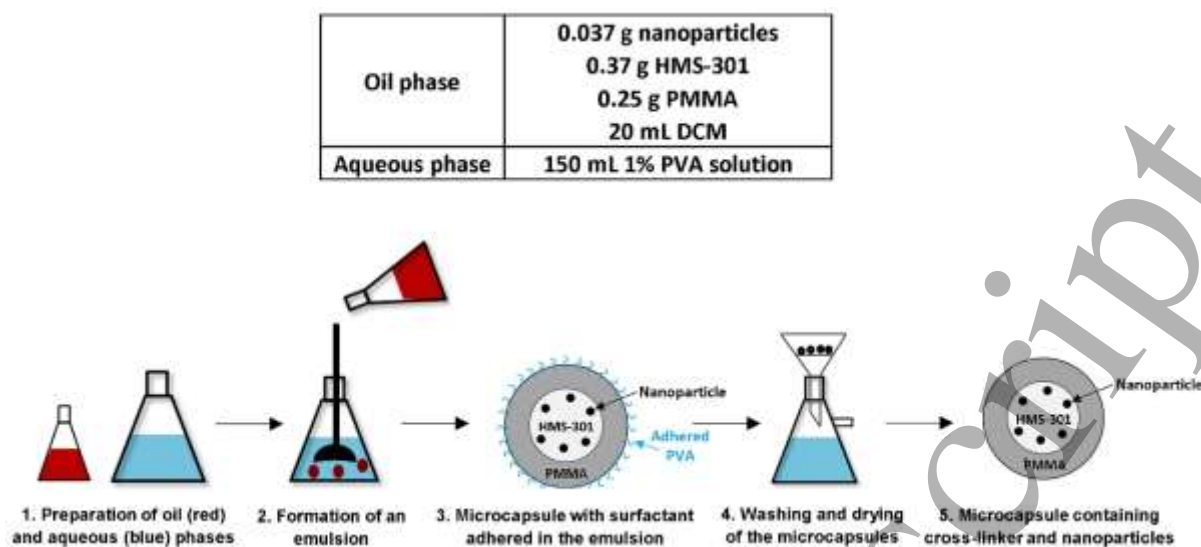


**Figure 2.** Schematic presentation of the phase separation technique. The table specifies particular conditions used during magnetic microcapsule preparation.

### 2.3. Preparation of vinyl-functional PDMS microspheres

Microspheres with vinyl groups on the surface were prepared using the emulsion method, as illustrated in **Figure 3**. First, a low-viscosity DMS-V22 premix, containing 50 ppm of Pt catalyst and 0.1% of the PT88 inhibitor, was prepared, following which a proper amount of the cross-linker (HMS-301) was added to the premix, in order to obtain a stoichiometric imbalance equal to  $r=0.8$ . A stoichiometric imbalance in this case is the ratio between the number of hydride groups to the number of vinyl groups, which means that mixtures with a stoichiometric imbalance lower than 1 have an excess of vinyl groups. This prepared mixture was then mixed for 2 minutes at 2000 rpm, using a SpeedMixer (FlackTek Inc. DAC 150.1 FVZ-K). Next, the mixture was added to approximately 200 mL of aqueous surfactant solution (1wt.% of PVA and 3wt.% of SDS) and stirred mechanically at 2000 rpm for 2 minutes, following which the speed was decreased to 750 rpm and the reaction carried out at 80 °C for 3 hours. Finally, the microspheres were washed with deionised water and dried at room temperature. Further

preparation details and characterisation of the PDMS microspheres are reported previously [25].

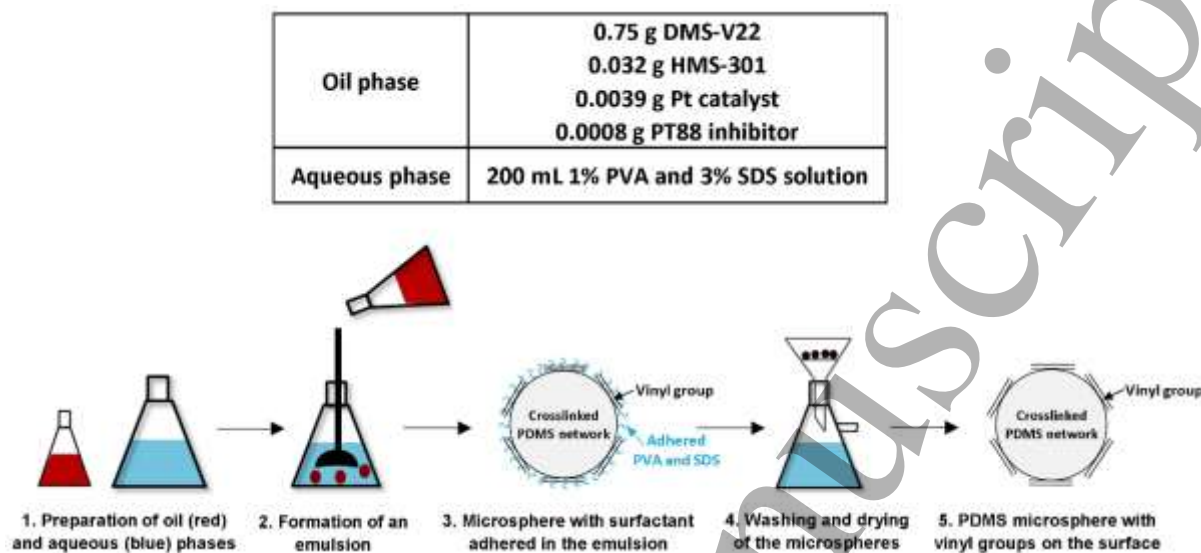


**Figure 3.** Schematic presentation of the emulsion method. The table specifies particular conditions used during microsphere preparation.

#### 2.4. Preparation of cross-linked plugging samples

The magnetic microcapsules and the vinyl-functional microspheres were physically mixed using a SpeedMixer with various mass ratios (1:10, 1:20, and 1:30). The mixture samples were heat-treated by AMF with different frequencies, which was performed using a MagneTherm instrument (Nanotherics). The samples were placed in the centre of a 17-loop induction coil. A non-contact IR thermometer (Fluke VT04 Visual) was used to detect temperature changes in the samples during the AMF treatment, which were performed in three cycles of 20 minutes, to avoid overheating the induction coil. Due to release of the cross-linker at temperatures higher than the  $T_g$  of the PMMA shell in the magnetic microcapsules, a cross-linking reaction would take place with the vinyl-functional microspheres.

## 2.5. Analytical methods

Optical microscopy images were taken using a portable Dino-Lite Edge digital microscope AM4115ZT (Dunwell Tech, Inc, USA). Scanning electron microscopy (SEM) images were recorded on an FEI Quanta 200 SEM (Thermo Fisher Scientific, USA) on samples coated with 2 nm-thick gold, using a Cressington 208HR sputter coater (Cressington Scientific Instruments, UK). Cryo-SEM was operated to show the cross-section of a PMMA microcapsule. The microcapsule sample was plunge frozen in liquid nitrogen on the cryo-stage of SEM and fractured in order to produce a fresh cross-section. The frozen fractured microcapsule was kept at  $\sim -140$  °C below the glass transition temperature of the core liquid HMS-301 ( $\sim -120$  °C) and imaged with an electron beam accelerated to the equilibrium voltage observed by SEM.

Thermogravimetric analysis (TGA) was performed using a TGA Discovery instrument (TA Instruments, USA), ranging from 20 °C to 800 °C with a heating rate of 10 °C/min in an N<sub>2</sub> atmosphere. The T<sub>g</sub> of the shell polymer PMMA was measured by employing differential scanning calorimetry (DSC) (Discovery, TA Instruments, USA) in the range of 0 °C to 150 °C at heating/cooling rates of 10 °C/min in an N<sub>2</sub> atmosphere. T<sub>g</sub> was calculated by a second heating scan, as the temperature of the halfway point of the jump in heat capacity when the material changed from a glassy to a rubbery state. <sup>1</sup>H NMR characterisation was performed on a Bruker 250 MHz spectrometer (Bruker, Germany), using CDCl<sub>3</sub> as a solvent. All spectra were recorded across 32 scans. Rheological measurements of the cross-linking behaviour were carried out in an inert nitrogen atmosphere, using a strain-controlled shear rheometer (ARES-G2, TA instruments, USA) set to a controlled strain mode with 2% strain, which was ensured to be within the linear regime of the material based on an initial strain sweep test. Time-resolved dynamic-mechanical mixture experiments were performed at a constant frequency of 1 Hz by applying a parallel plate geometry of 25 mm in diameter and a gap of 1 mm at 50 °C and 90 °C. The linear visco-elastic (LVE) data for the cross-linked samples were measured

with parallel-plate geometry of 25 mm at a diameter of 23 °C. The LVE diagrams were obtained from frequency sweeps ranging from 100 Hz to 0.01 Hz. A non-contact VT04 Visual IR thermometer (Fluke, USA) was used to detect temperature changes in the samples during the AMF treatment by a MagneTherm instrument (Nanotherics, UK).

### 3. Results and discussion

#### 3.1. Activation of the magnetite nanoparticles in AMF

Figures 4a and b present SEM images of the magnetite nanoparticles  $\text{Fe}_3\text{O}_4$  without and with PDMS surface modification, respectively. The particles were spherical and their diameters were between 20 and 60 nm.

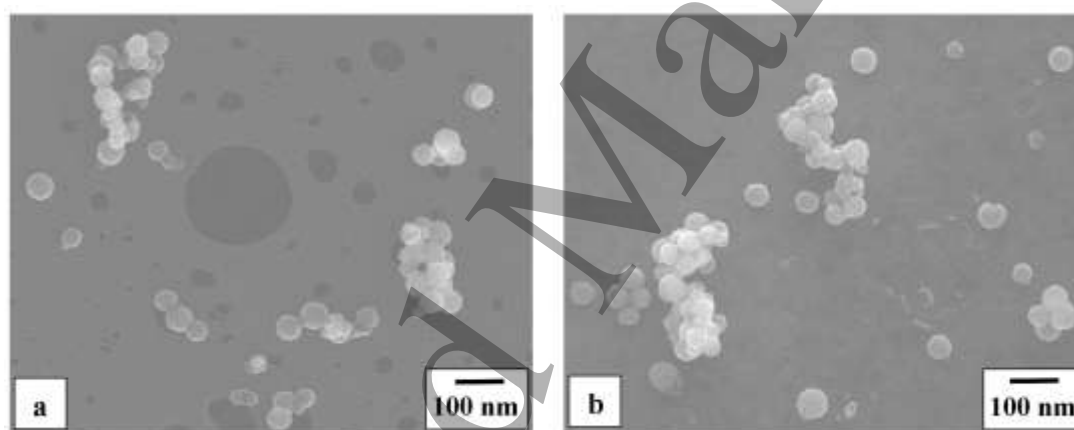
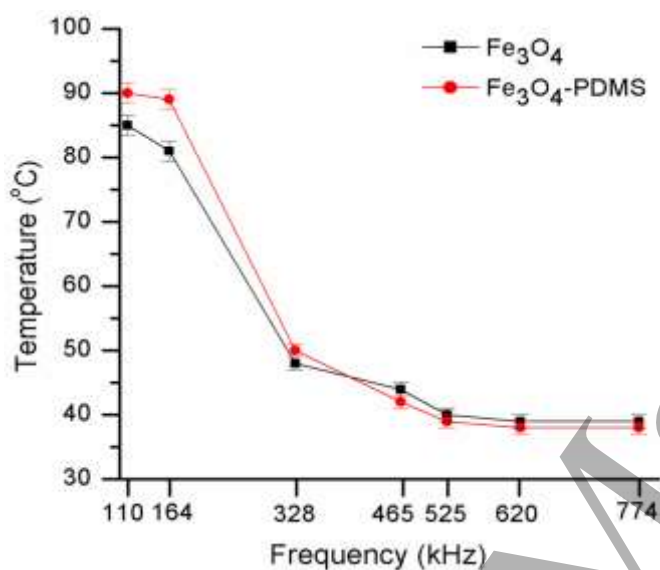


Figure 4. SEM pictures of magnetite nanoparticles. a)  $\text{Fe}_3\text{O}_4$ . b)  $\text{Fe}_3\text{O}_4$ -PDMS.

When the polymer mixtures incorporating MNPs were exposed to the AMF, the MNPs dissipated the energy to the surrounding matrix, due to friction between the oscillating magnetic particles and the stationary matrix [16]. Consequently, AMF generates heat rapidly and locally, compared to supplying heat directly to thermally insulating materials, e.g. silicone [14]. In order to determine which type of MNP can generate sufficient heat to soften the PMMA shell, aqueous mixtures with 5% MNP mass content were prepared and exposed to AMF for

20 minutes at various frequencies, since the thermal response of the magnetic composite through exposure to an AMF depends on the frequency of the magnetic field [26]. A frequency-response profile of magnetic particles dispersed in the aqueous mixtures is presented in **Figure 5**. The available nominal frequencies of MagneTherm instrument are noted on the x-axis. The highest temperatures were obtained at a frequency of 110 kHz for both MNPs.



**Figure 5.** AMF frequency-dependent temperature elevation of the aqueous mixtures with a 5%-mass content of MNPs. The two different MNPs was examined by the exposure to the AMF for 20 minutes at various frequencies. The error bars were calculated from the triplicate measurements.

In **Figure 5**, the mixture containing 5wt.% of Fe<sub>3</sub>O<sub>4</sub>-PDMS nanoparticles reaches the highest temperature of all mixtures at 90 °C at 110 kHz, showing the possibility of melting the PMMA shell with  $T_g$  equal to 88°C (**Figure S1**). According to the quantitative analysis of magnetic microcapsules by TGA and NMR (**ESI**), MNPs constituted more than 30% of the core mass. Therefore, during exposure to the AMF, the encapsulated nanoparticles were able to generate sufficient heat to increase the temperature higher than 90 °C and thereby soften the

1  
2  
3 PMMA shell, thus allowing for the efficient release of the liquid cross-linker. However, it was  
4  
5 shown that the mixture with Fe<sub>3</sub>O<sub>4</sub> nanoparticles reached 85 °C at 110 kHz, thereby indicating  
6  
7 that the PMMA shell might not be softened enough by the application of the AMF because the  
8  
9 generated temperature was lower than the T<sub>g</sub> of PMMA (88 °C).  
10  
11  
12  
13  
14

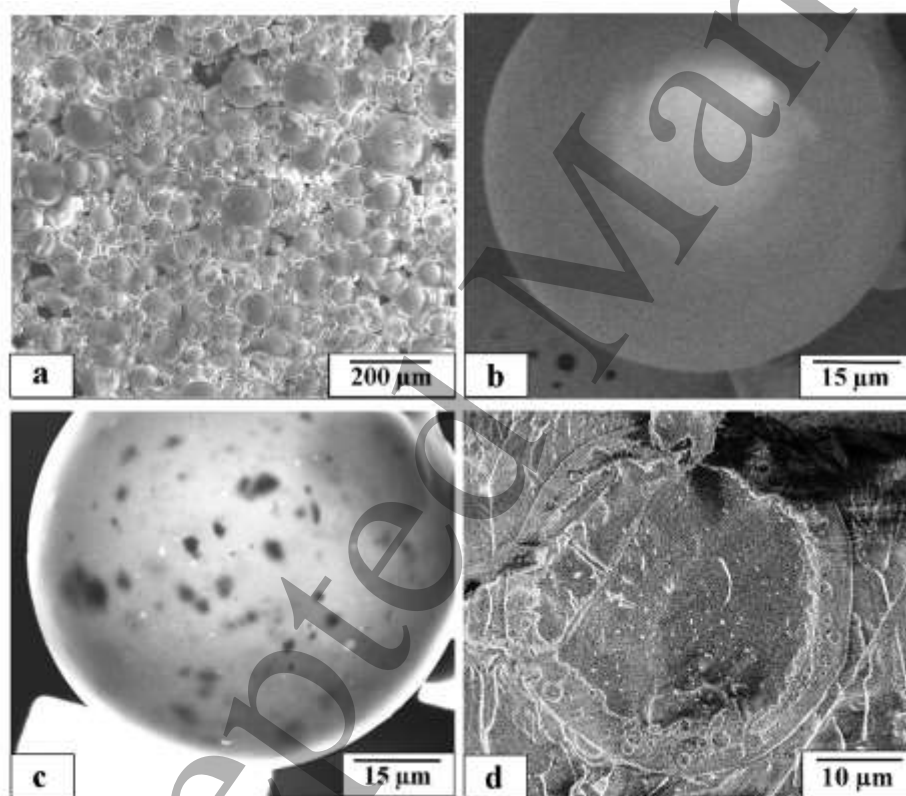
### 15 **3.2. Microscopical characterisation of the magnetic microcapsules**

16  
17 As the MNP Fe<sub>3</sub>O<sub>4</sub> exhibited sufficient heat generation under an AMF with a frequency of 110  
18  
19 kHz to make the PMMA soft, as well its well-dispersion in the hydrophobic cross-linker due  
20  
21 to the PDMS surface modification, it was selected to be encapsulated together with a liquid  
22  
23 cross-linker via the phase separation technique, following the procedure given in the  
24  
25 experimental chapter.  
26  
27

28  
29 **Figures 6a** and **b** present the secondary electron (SE) images of the microcapsules with  
30  
31 Fe<sub>3</sub>O<sub>4</sub>-PDMS nanoparticles. All the microcapsules were spherical and their diameter fell  
32  
33 between 20 and 150 μm (**Figure 6a**). It is obvious that no nanoparticles or pores were present  
34  
35 on the shell's surface (**Figure 6b**). The continuous surface shows that the PMMA shell  
36  
37 encapsulated successfully the cross-linker which is located at the core. **Figure 6c** presents a  
38  
39 microcapsule imaged in bright-field scanning transmission electron microscopy (STEM) mode  
40  
41 of SEM. The SE imaging is sensitive to the surface topography, while the STEM imaging is in  
42  
43 projection along an electron beam, which allows the internal structure of a specimen to be  
44  
45 imaged at relatively high resolution. The comparison of the two images suggests that dark  
46  
47 contrast in the STEM corresponds to MNPs that are located inside the microcapsule. It is noted  
48  
49 that these visible MNPs would be the aggregation of nanometer-sized MNPs as shown in  
50  
51 **Figure 4b**. **Figure 6d** shows a cross-section of a microcapsule, which was acquired at a  
52  
53 temperature (~-140 °C) below the glass transition temperature of the crosslinker, HMS-301.  
54  
55  
56  
57  
58

59 The image clearly shows a core/shell structure, which is composed of the crosslinker (core)  
60

1  
2  
3 and ~5- $\mu\text{m}$ -thick PMMA (shell). The interface between the crosslinker and the PMMA is rather  
4 rough, while the outer surface of the PMMA shell is smooth, which can also be observed in the  
5  
6 SE image shown in **Figure 6b**. The MNPs are located only in the crosslinker with relatively  
7 well dispersion, indicating that a temperature rise induced by AFM may occur uniformly in the  
8 crosslinker. Although various sized pores with up to 2  $\mu\text{m}$  are present in the PMMA shell, the  
9 pores have smaller sizes than the shell thickness and are not exposed to the surface. Therefore,  
10 the crosslinker inside the microcapsules would not be released to the outside as it is. When  
11 AMF is applied to the MNPs dispersed in the microcapsules, the MNPs would produce  
12 sufficient heat to soften the PMMA shell and release the cross-linker from the microcapsules.  
13  
14  
15  
16  
17  
18  
19  
20  
21  
22  
23  
24  
25  
26  
27  
28  
29  
30  
31  
32  
33  
34  
35  
36  
37  
38  
39  
40  
41  
42  
43  
44  
45  
46  
47  
48  
49  
50  
51  
52



53 **Figure 6.** SEM photographs of microcapsules containing the  $\text{Fe}_3\text{O}_4$ -PDMS nanoparticles. **a)**  
54 Low magnification SE image of a microcapsule aggregation. **b)** and **c)** SE and bright-field  
55 STEM images of a single microcapsule. The images **b)** and **c)** were acquired from the same  
56  
57  
58  
59  
60

microcapsule. Dotted-like bright contrast in **c**) corresponds to pores in the shell. **d**) SE image of a cross-section of a microcapsule obtained around  $-140\text{ }^{\circ}\text{C}$  by cryo-SEM.

### 3.3. Cross-linked plugging samples containing magnetic microcapsules and PDMS microspheres

Magnetic microcapsule reactivity was investigated by means of rheology. The microcapsules were mixed with the PDMS premix with a mass ratio 1:10, which was shown previously to be the suitable ratio to obtain a strong low-loss tangent ( $\text{Tan}\delta < 0.1$  @ 1 Hz) network [27]. The PDMS premix consisted of the vinyl-terminated poly(dimethylsiloxane) DMS-V31 with 50 ppm of a platinum catalyst. Two identical mixtures were then investigated at different temperatures, and the storage modulus ( $G'$ ) and loss modulus ( $G''$ ) are presented in **Figure 7**.

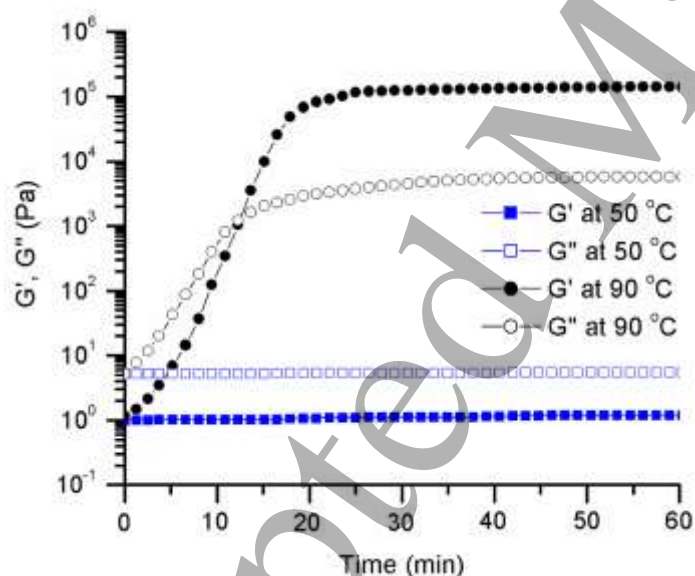


**Figure 7.** Development of storage and loss moduli ( $G'$  and  $G''$ ) of the mixtures containing a PDMS premix (DMS-V31 with platinum catalyst) and magnetic microcapsules. The measurements were performed at 1 Hz at  $50\text{ }^{\circ}\text{C}$  and  $90\text{ }^{\circ}\text{C}$  controlled by rheometer, respectively, for 1 hour.



1  
2  
3 The performed tests showed that the magnetic microcapsules were impermeable at 50 °C  
4 heated by rheometer oven, as both moduli remained constant over time during the one-hour  
5 experiment.  $G''$  (loss modulus) was higher than  $G'$  (storage modulus) during the entire  
6 measurement phase, implying that the cross-linker was not released and therefore the cross-  
7 linking reaction was not initiated. At 90 °C, as expected, the PMMA became soft and pliable,  
8 and the microcapsules disintegrated, thereby releasing the cross-linker. This led to the  
9 formation of the three-dimensional network of vinyl-terminated PDMS reacted with hydride-  
10 functional cross-linker and a subsequent increase in the storage modulus, which reached a  
11 plateau after approximately 20 minutes, with values significantly higher than the loss modulus,  
12 thus confirming the formation of the strong PDMS network. Furthermore, gelation was  
13 achieved at around 13 minutes.  
14  
15  
16  
17  
18  
19  
20  
21  
22  
23  
24  
25  
26  
27

28 After identifying the reactivity of the magnetic microcapsules at 90 °C, the cross-linked  
29 plugging samples made from the vinyl-functional PDMS microspheres and the magnetic  
30 microcapsules were examined. As seen in **Figure 7**, at 90°C the dynamic moduli  $G'$  and  $G''$   
31 reached steady state after 1 hour, so AMF experiments were performed in three cycles of 20  
32 minutes to avoid overheating the induction coil. **Figure 8** shows a schematic presentation and  
33 microscopic images of the magnetic microcapsules and the PDMS microspheres (mixed mass  
34 ratio 1:10), before and after the cross-linking reaction. Before the reaction, the PDMS  
35 microspheres were not connected to each other. The cross-linker was released after exposing  
36 microcapsules with  $\text{Fe}_3\text{O}_4$ -PDMS nanoparticles to AMF at 110 kHz for an hour. Non-reactive  
37 silicone oil with a platinum catalyst was used as a reaction matrix to enable a hydrosilylation  
38 reaction between the PDMS microspheres and the released cross-linker. After the reaction, the  
39 PDMS microspheres were connected through inter-spherical covalent bonds [28].  
40  
41  
42  
43  
44  
45  
46  
47  
48  
49  
50  
51  
52  
53  
54  
55  
56  
57  
58  
59  
60

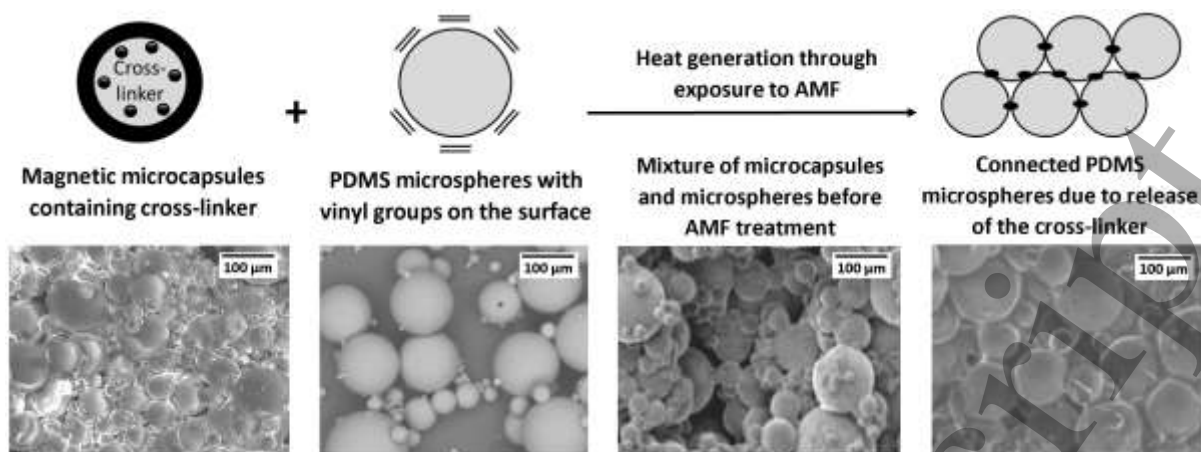
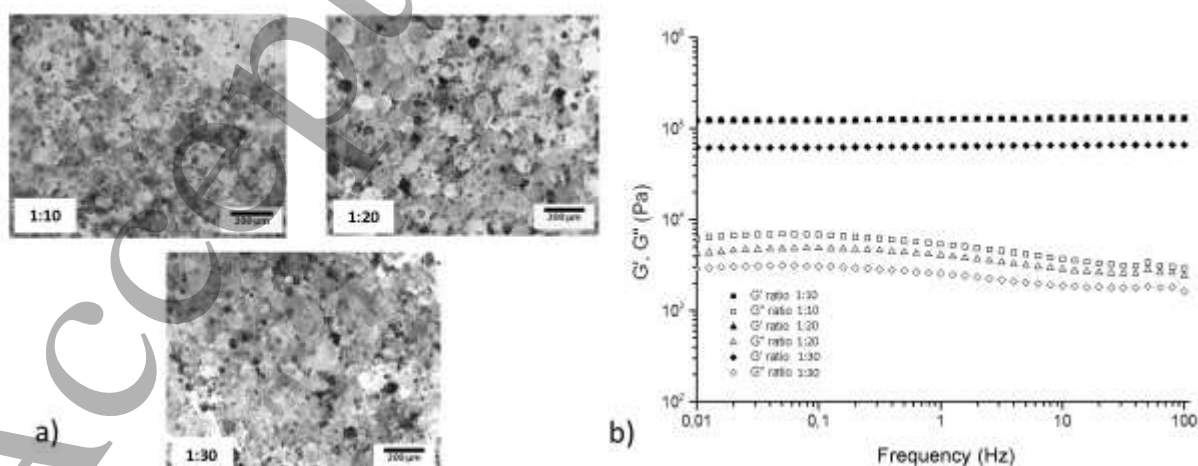


**Figure 8.** Schematic presentation and SEM images of the magnetic microcapsules and the PDMS microspheres, before and after the cross-linking reaction.

**Figure 9a** shows optical microscopy images of the cross-linked plugging samples with different microcapsule-to-PDMS microsphere mass ratios. Since the microcapsules contained MNPs, distinguishing them from the microspheres is possible between portions of bright microspheres and dark MNPs. It is evident that the microcapsules were dispersed well within the sample through the speed mixing treatment, without the occurrence of obvious agglomerations, thereby resulting in the homogeneous distribution of a released cross-linker. When the cross-linker is spread uniformly, the cross-linking density of PDMS microspheres is similar throughout the whole volume and therefore leads to the formation of a uniform network.



1  
2  
3 **Figure 9.** Morphology and viscoelasticity of the cross-linked plugging samples containing  
4 magnetic microcapsules and vinyl-functional PDMS microspheres. **a)** Optical microscopy  
5 images. **b)** The storage ( $G'$ ) and the loss ( $G''$ ) moduli as a function of applied frequency. The  
6 mass ratios of the microcapsule to the microsphere are stated on the images and graph.  
7  
8  
9

10  
11  
12  
13  
14  
15 From frequency sweep tests, the storage ( $G'$ ) and the loss moduli ( $G''$ ) of the cross-linked  
16 plugging samples with various magnetic microcapsule-to-PDMS microspheres ratios were  
17 measured, as seen in **Figure 9b**. In three different storage moduli curves, the values of  $G'$  were  
18 independent of the frequency, meaning that the released liquid cross-linker took part in a  
19 hydrosilylation reaction and led to covalent bonding between the PDMS microspheres.  
20  
21 Moreover, despite the fact that the cross-linked sample was formed from individual  
22 microspheres, it can be considered a uniform and well-organised material. Furthermore, the  
23 values of  $G'$  for three samples were very similar, the samples with the ratios 1:10 and 1:20 had  
24 an almost identical storage modulus, whereas the sample with the 1:30 ratio had only a slightly  
25 lower  $G'$ . This proved that regardless of the ratio between the compounds, the cross-linked  
26 samples showed similar mechanical properties, thus demonstrating that deviations in ratios  
27 between the compounds (within the tested range) will not have a negative impact on the final  
28 properties of the plug inside the fracture, and thus the sensitivity of the system on the mixing  
29 ratio is low.  
30  
31  
32  
33  
34  
35  
36  
37  
38  
39  
40  
41  
42  
43  
44  
45  
46  
47  
48

#### 49 **4. Conclusions**

50  
51 A cross-linked plugging material consisting of magnetically activated microcapsules and vinyl-  
52 functional PDMS microspheres was prepared successfully. Encapsulating the cross-linker  
53 provided control over the cross-linking reaction between the vinyl-functional microspheres,  
54 whereas incorporating magnetite nanoparticles (MNPs) into the microcapsules' structure  
55  
56  
57  
58  
59  
60

1  
2  
3 introduced the possibility of remote activation by applying the alternating magnetic field  
4 (AMF). While applying AMF, the MNPs generated heat, and a 5wt.% aqueous mixture of the  
5  $\text{Fe}_3\text{O}_4$  nanoparticles with a PDMS surface modification at 110 kHz reached 90 °C higher than  
6 the  $T_g$  (88 °C) of the PMMA shell. The obtained magnetic microcapsules, prepared via the  
7 phase separation technique, contained high amounts of the MNPs (>15wt.%), which were  
8 located inside the microcapsules. The structure of the PMMA shell was not influenced by the  
9 presence of the MNPs and remained non-porous; hence, the magnetic microcapsules were  
10 impermeable at temperatures lower than the  $T_g$  of the shell, and the cross-linker was separated  
11 fully from the environment until microcapsule activation. This notion was proved by mixing  
12 the microcapsules with vinyl-terminated PDMS, and the cross-linking reaction was observed  
13 only at temperatures higher than the  $T_g$  of the shell. Moreover, vinyl-functional PDMS  
14 microspheres mixed with the magnetic microcapsules created a strong network after the cross-  
15 linking reaction. The microcapsules were distributed uniformly within the whole volume of the  
16 network, thus enabling good bonding between the microspheres. It was presented that  
17 deviations in the mass ratio between the magnetic microcapsules and the PDMS microspheres  
18 did not influence the elastic properties of the cross-linked sample, which is of great importance  
19 regarding application in oil recovery treatments, where the mass ratio cannot be controlled  
20 precisely.  
21  
22  
23  
24  
25  
26  
27  
28  
29  
30  
31  
32  
33  
34  
35  
36  
37  
38  
39  
40  
41  
42  
43  
44  
45  
46

### 47 **Acknowledgements**

48  
49 The authors wish to express our thanks to Ramona Valentina Mateiu (Hempel Foundation  
50 Coatings Science and Technology Center, DTU) for invaluable discussion on the SEM  
51 investigation. The authors gratefully acknowledge Mærsk Oil & Gas Research, Qatar for the  
52 financial support and the A.P. Møller and Chastine Mc-Kinney Møller Foundation for the  
53  
54  
55  
56  
57  
58  
59  
60

1  
2  
3 contribution towards the establishment of the Center for Electron Nanoscopy in the Technical  
4  
5 University of Denmark.  
6  
7  
8  
9

## 10 **References**

- 11  
12 [1] Hadia N, Chaudhari L, Mitra S K, Viniamur M and Singh R 2007 *J. Pet. Sci. & Eng.* **56**  
13  
14 303  
15  
16 [2] Kok M V 2011 *Energy Sources, Part A Recover. Util. Environ. Eff.* **33** 377  
17  
18 [3] Marescalco P A C 2008 *Int. J. Numer. Methods Fluids* **61** 768  
19  
20 [4] Bai B, Zhou J and Yin M 2015 *Pet. Explor. Dev.* **42** 525  
21  
22 [5] Oglesby K D, D'Souza D, Roller C, Longsdon R, Burns L D and Felber B J 2016 *SPE*  
23  
24 *Improved Oil Recovery Conference held in Tulsa, USA* 1-25  
25  
26 [6] Hassan S F, Han M, Zhou X, Krinis D, Zahrani B and Aramco S 2013 *SPE Annual*  
27  
28 *Technical Symposium and Exhibition held in Khobar, Saudi Arabia* 1-11  
29  
30 [7] Simjoo M, Koohi A D, Vafaie-Sefti M and Zitha P L J 2009 *SPE European Formation*  
31  
32 *Damage Conference held in Scheveningen, The Netherlands* 1-8  
33  
34 [8] Al-Muntasheri G A, Sierra L, Garzon F O, Lynn J D and Izquierdo G 2010 *SPE Improved*  
35  
36 *Oil Recovery Symposium held in Tulsa, USA* 1-24  
37  
38 [9] Ryles R and Cicchiello J 1986 *SPE/DOE Fifth Symposium on Enhanced Oil Recovery of the*  
39  
40 *Society of Petroleum Engineers of the Department of Energy held in Tulsa, USA* 301-305  
41  
42 [10] Madsen F B, Daugaard A E, Hvilsted S and Skov A L 2016 *Macromol. Rapid Commun.*  
43  
44 **37** 378  
45  
46 [11] Larsen A L, Hansen K, Sommer-Larsen P, Hassager O, Bach A, Ndoni S and Jørgensen  
47  
48 M 2003 *Macromolecules* **36** 10063  
49  
50 [12] Vaishnava P P, Tackett R, Dixit A, Sudakar C, Naik R and Lawes G 2007 *J. Appl. Phys.*  
51  
52 **102** 63914  
53  
54  
55  
56  
57  
58  
59  
60

- 1  
2  
3 [13] Tomitaka A, Ueda K, Yamada T and Takemura Y 2012 *J. Magn. Magn. Mater.* **324** 3437  
4  
5 [14] Regmi R, Naik A, Thakur J S, Vaishnava P P and Lawes G 2014 *J. Appl. Phys.* **115**  
6  
7 17B301  
8  
9 [15] Suto M, Hirota Y, Mamiya H, Fujita A, Kasuya R, Tohji K and Jeyadevan B 2009 *J.*  
10  
11 *Magn. Magn. Mater.* **321** 1493  
12  
13 [16] Ogliani E, Yu L, Javakhishvili I and Skov A L 2018 *RSC Adv.* **8** 8285  
14  
15 [17] Li J, Gu J, Li H, Liang Y, Hao Y, Sun X and Wang L 2010 *Micropor. Mesopor. Mat.* **128**  
16  
17 144  
18  
19 [18] Pan S, Li J, Wan G, Liu C, Fan W and Wang L 2016 *J. Hazard. Mater.* **309** 1  
20  
21 [19] Gleich B and Weizenecker J 2005 *Nature* **435** 1214  
22  
23 [20] Krishnan K M 2010 *IEEE Trans. Magn.* **46** 2523  
24  
25 [21] Chung S H, Hoffmann A and Bader S D 2004 *Appl. Phys. Lett.* **85** 2971  
26  
27 [22] Liu J, Sun Z, Deng Y, Zou Y, Li C, Guo X, Xiog L, Gao Y, Li F and Zhao D 2009 *Angew.*  
28  
29 *Chem. Int. Ed.* **48** 5875-5879  
30  
31 [23] González L, Kostrzewska M, Ma B, Li L, Hansen J H, Hvilsted S and Skov A L 2014  
32  
33 *Macromol. Mater. Eng.* **299** 1259  
34  
35 [24] Ma B, Hansen J H, Hvilsted S and Skov A L 2014 *RSC Adv.* **4** 47505  
36  
37 [25] González L, Ma B, Li L, Hansen J H, Hvilsted S and Skov A L 2014 *Macromol. Mater.*  
38  
39 *Eng.* **299** 729  
40  
41 [26] Hohlbein N, Shaaban A and Schmidt A M 2015 *Polymer* **69** 301-309  
42  
43 [27] Kostrzewska M, Ma B, Javakhishvili I, Hansen J H, Hvilsted S and Skov A L 2015 *Polym.*  
44  
45 *Adv. Technol.* **26** 1059  
46  
47 [28] Brook M A *Silicon in Organic, Organometallic, and Polymer Chemistry* 2000 John Wiley  
48  
49 & Sons, New York, United States  
50  
51  
52  
53  
54  
55  
56  
57  
58  
59  
60